Improving Power Utilization Factor of Broadband Doherty Amplifier by Using Bandpass Auxiliary Transformer

Xiao-Hu Fang, *Student Member, IEEE*, and Kwok-Keung M. Cheng, *Senior Member, IEEE*

***Abstract*—In this paper, a novel Doherty power amplifier (DPA) configuration with an auxiliary transformer is proposed for broadband operation. Theoretical analysis reveals that the proposed design can offer enhanced power utilization factor (PUF) and wideband Doherty behavior. The optimal design of the auxiliary transformer is identified with an aim to provide good impedance matching and minimal group delay. Based on the proposed theory, a 1.6–2.4-GHz 20-W DPA with improved PUF is designed, simulated, and measured. Under continuous wave excitation, measurement results indicate that the proposed DPA can achieve a PUF of 0.9, good Doherty behavior over the entire frequency band with a 6-dB back-off efficiency of 55%–64%, and saturated efficiency of 68%–76%. In addition, by the use of single-carrier WCDMA signal (centered at 2 GHz) with peak-to-average power ratio of 6.6 dB and at an average output power of 37 dBm, an average drain efficiency of 56% is obtained with adjacent channel leakage power ratio of better than −37 dBc.**

***Index Terms*—Auxiliary transformer, bandpass, broadband, Doherty power amplifier (DPA), efficiency, power utilization factor (PUF).**

I. Introduction

As MODERN communication system demands higher spectrum efficiency and data rate, new communication standard using a complex modulation scheme has emerged and led to transmitting signal with ever-increasing peak-to-average power ratio (PAPR). Moreover, the coexistence of different standards requires RF transceivers to support signal transmission at multiple carrier frequencies. Therefore, wideband operation and efficient amplification of the high PAPR signal are prime requirements for base-station power amplifier (PA) design. Besides, the microwave power transistor is usually considered to be the most expensive component in PA construction, and therefore the full utilization of the device capacity (PUF $= 1$) is highly desirable.

For efficiency enhancement, the Doherty power amplifier (DPA) [1] has been regarded as the most popular approach due to its circuit simplicity and moderate linearity [2]–[15].

Manuscript received September 19, 2014; revised January 27, 2015 and June 09, 2015; accepted June 13, 2015. Date of publication July 07, 2015; date of current version September 01, 2015.

The authors are with the Department of Electronic Engineering, The Chinese University of Hong Kong, Shatin, NT, Hong Kong (e-mail: xhfang@ee.cuhk.edu.hk; kkcheng@ee.cuhk.edu.hk).

Color versions of one or more of the figures in this paper are available online at http://ieeexplore.ieee.org.

Digital Object Identifier 10.1109/TMTT.2015.2447544

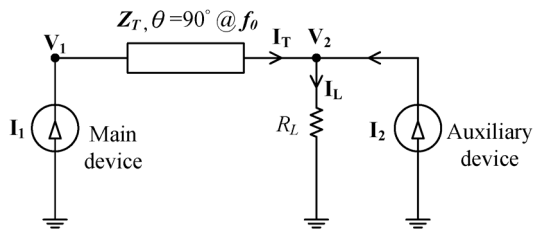

Fig. 1. Simplified schematic of DPA.

Fig. 1 shows a generic diagram of the DPA. In the low-power region (auxiliary device is off), the Main device operates as a normal PA with a fixed load impedance. When the auxiliary device is on (Doherty region), the effective load seen by the Main amplifier is dynamically modulated and a high level of efficiency is maintained over a specific range of power back-off. The classical design with $Z_T = 2R_L = R_{\rm opt}$ ($R_{\rm opt}$ is the optimum load impedance of power devices), which is widely used in the implementation of the narrowband DPA [2], employs identical Main and Auxiliary devices, with a theoretical PUF of unity and output back-off (OBO) range of 6 dB. In theory, this DPA configuration can achieve high efficiency at saturation over a wide frequency band. However, the back-off efficiency degrades substantially [3]–[5] due to the narrowband nature of the simple quarter-wavelength transformer. In [6], a sub-optimal value of Z_T was selected to attain wideband operation with some compromise between saturation and back-off efficiencies. In [7] and [8], a modified configuration ($Z_T = R_L = 2R_{\rm opt}$), with an aim to improve back-off efficiency and bandwidth, was introduced at the expense of PUF $(= 0.5)$. A mixed-technology DPA was also described [9] to slightly restore the value of PUF $(= 0.66)$ by having asymmetrical devices of different breakdown voltages. Meanwhile, for wideband operation, it is well known that the frequency dispersion of the auxiliary matching network is a major limiting factor. In [7]–[9], a DPA design without an auxiliary matching network was presented to minimize dispersion, with the major drawback of degraded efficiency and power performance.

In this paper, a novel DPA design based on an auxiliary transformer is proposed. By inserting a transformer into the output matching network of the auxiliary amplifier, ideal PUF condition and broadband Doherty behavior can be achieved simultaneously. Moreover, the optimum design of the auxiliary matching network based upon bandpass topology is also addressed to minimize the impact of frequency dispersion.

For validation, both the simulated and measured results of a 1.6–2.4-GHz 20-W DPA with 6-dB back-off efficiency of over 55% and saturation efficiency of around 72% are demonstrated.

II. Theory

For the sake of analyses, the following assumptions are adopted.

1) Ideal device model with zero knee voltage and parasitic. In other words, the optimum drain load for maximum output power is purely resistive.
2) Symmetrical DPA (identical main and auxiliary devices) is employed with the same upper limits on breakdown voltage and current rating ($V_{\rm MAX}$ and $I_{\rm MAX}$). Both devices are operating in Class-B mode.
3) All higher voltage harmonics are short circuited and only the fundamental component is retained.
4) All matching networks are lossless and reciprocal.

A. PUF of Conventional DPA Configurations

Referring to Fig. 1, by using $ABCD$-parameter representation, the relation between the drain voltages and currents of the main and auxiliary devices can be formulated as

$$\begin{bmatrix} \mathbf{V_1} \\ \mathbf{I}_1 \end{bmatrix} = \begin{bmatrix} \dfrac{jZ_T}{R_L} & jZ_T \\ \dfrac{j}{Z_T} & 0 \end{bmatrix} \begin{bmatrix} \mathbf{V_2} \\ -\mathbf{I_2} \end{bmatrix}. \tag{1}$$

With an OBO range of 6 dB, the load impedance of the main device under low-power operation (i.e., $I_2 = 0$) is given by (2), where $R_{\rm opt}$ denotes the optimum load impedance of the Main device for a given dc bias voltage and saturation current level,

$$\frac{Z_T^2}{R_L} = 2R_{\rm opt}. \tag{2}$$

Furthermore, by combining (1) and (2), with the assumption that $\mathbf{I}_2$ lags $\mathbf{I}_1$ by 90°, the magnitudes of the saturation voltages and currents can simply be related as

$$V_{2\rm sat} = \frac{2R_L}{Z_T} V_{1\rm sat} \tag{3}$$

$$I_{2\rm sat} = \frac{Z_T}{2R_L} I_{1\rm sat}. \tag{4}$$

According to [9], the PUF is defined by the ratio between the maximum output power of the DPA and the two active devices (Class-B operation is assumed)

$$\text{PUF} = \frac{P_{\rm max,DPA}}{P_{{\rm max},M} + P_{{\rm max},A}} = \frac{4V_{2\rm sat}I_{2\rm sat}}{V_{\rm MAX}I_{\rm MAX}}. \tag{5}$$

Subsequently, with $Z_T = 2R_L$ (classical DPA design), the main and auxiliary devices are expected to have the same saturation voltage ($V_{1\rm sat} = V_{2\rm sat}$) and current ($I_{1\rm sat} = I_{2\rm sat}$) levels. Therefore, with an appropriate selection of drain bias ($= 0.5V_{\rm MAX}$), the power capacity of both devices can be fully deployed (PUF $= 1$). However, as suggested in [7] and [8], this configuration is not suitable for broadband operation since the adopted quarter-wavelength transformer is band-limited and severe degradation in efficiency and output power can be observed. To maintain high performance over a wide bandwidth, a different choice of characteristic impedance ($Z_T = R_L$) was suggested. Under low-power operation (below the first efficiency peak), the load impedance seen by the main device is inherently independent of frequency ($= 2R_{\rm opt}$). Unfortunately, according to (3) and (4), the saturation voltages and currents of the main and auxiliary devices will become unequal (i.e., $V_{2\rm sat} = 2V_{1\rm sat}$; and $I_{2\rm sat} = 0.5I_{1\rm sat}$). In other words, the bias voltage of the main device has to be substantially reduced ($V_{1\rm sat} = 0.25V_{\rm MAX}$), while only half of the current capacity of the auxiliary device ($I_{2\rm sat} = 0.25I_{\rm MAX}$) is exploited. In consequence [9], this broadband topology performs sub-optimally with reduced PUF ($= 0.5$).

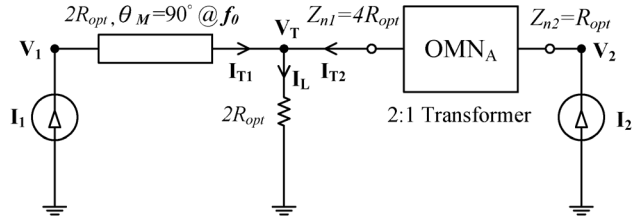

Fig. 2. Proposed DPA configuration with auxiliary transformer.

B. Enhanced PUF by Using Auxiliary Transformer

To improve the PUF, a transformer is introduced into the auxiliary branch, as depicted in Fig. 2. With the specific voltage ratio (2:1) of the transformer, the saturation voltages and currents of both devices are maximized (i.e., $V_{1\rm sat} = V_{2\rm sat} = 0.5\,V_{\rm MAX}$; and $I_{1\rm sat} = I_{2\rm sat} = 0.5\,I_{\rm MAX}$). Therefore, the main and auxiliary devices can operate at full capacity (PUF $= 1$) while ideal Doherty behavior is maintained over an extended bandwidth.

In practice, ideal transformer (broadband and low loss) is not available at microwave frequencies. Therefore, an impedance transformer with pre-selected port impedances ($Z_{n1} = 4R_{\rm opt}, Z_{n2} = R_{\rm opt}$) is chosen to perform the required voltage scaling function. If the transmission phase response of the auxiliary transformer is denoted as θ_A ($\theta_A = 0$ only at f_0), its scattering-parameters can thus be expressed as follows [16]:

$$S_A = \begin{bmatrix} 0 & e^{-j\theta_A} \\ e^{-j\theta_A} & 0 \end{bmatrix}. \tag{6}$$

Accordingly, by using $ABCD$ parameters, the dependency between the terminal voltages and branch currents of the auxiliary transformer can simply be written as

$$\begin{bmatrix} \mathbf{V_T} \\ -\mathbf{I_{T2}} \end{bmatrix} = \begin{bmatrix} 2\cos\theta_A & j2R_{\rm opt}\sin\theta_A \\ \dfrac{j\sin\theta_A}{2R_{\rm opt}} & \dfrac{\cos\theta_A}{2} \end{bmatrix} \begin{bmatrix} \mathbf{V_2} \\ -\mathbf{I_2} \end{bmatrix}. \tag{7}$$

For further analysis, the transformer and the auxiliary current are replaced by its equivalent circuit, as depicted in Fig. 3(a). The mathematical expressions of the shunt reactance ($\mathbf{Z_{SA}}$) and the modified current source ($\mathbf{I_{SA}}$) are given by (8) and (9). Note that the frequency response of the shunt reactance is similar to that of a parallel-tuned circuit ($Z_{\mathbf{SA}} = \infty$ at f_0)

$$\mathbf{I_{SA}} = \frac{\mathbf{I_2}}{2\cos\theta_A} \tag{8}$$

$$\mathbf{Z_{SA}} = \frac{4R_{\rm opt}}{j\tan\theta_A}. \tag{9}$$

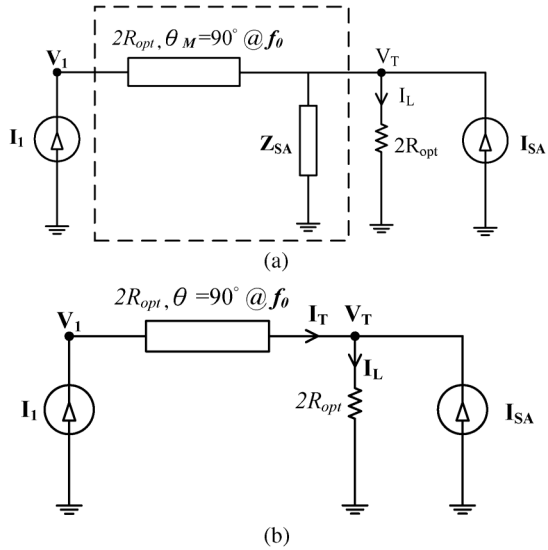

Fig. 3. Proposed DPA with nonideal transformer. (a) Simplified version. (b) Equivalent circuit.

To maintain broadband Doherty operation (first efficiency peak), the combined effect of TL_M (quarter-wavelength transmission line) and $\mathbf{Z_{SA}}$ is made equivalent to an ideal transmission line with characteristic impedance of $2R_{\mathrm{opt}}$ and electrical length of 90° (at f_0 only), as depicted in Fig. 3(b). Note that when the auxiliary device is off $(I_2 = 0)$, the circuits in Figs. 1 and 3(b) are basically identical. To a first approximation, the electrical length (θ) of the equivalent line can be evaluated by (10), where θ_M corresponds to the phase response of TL_M; while the second term represents the transmission phase introduced by the shunt reactance (auxiliary transformer)

$$\theta = \theta_M + \theta_A/2. \tag{10}$$

C. Optimal Phase Control for Broadband Operation

With reference to Fig. 3(b), by the multiplication of $ABCD$ matrices, the relation between the terminal voltages and branch currents can be obtained as

$$\begin{bmatrix} \mathbf{V_1} \\ \mathbf{I_1} \end{bmatrix} = \begin{bmatrix} e^{j\theta} & j2R_{\mathrm{opt}} \sin\theta \\ \dfrac{e^{j\theta}}{2R_{\mathrm{opt}}} & \cos\theta \end{bmatrix} \begin{bmatrix} \mathbf{V_T} \\ -\mathbf{I_{SA}} \end{bmatrix}. \tag{11}$$

Combining (8) and the second row of (11), we have

$$\mathbf{V_T} = R_{\mathrm{opt}} \left(2\mathbf{I_1} + \frac{\mathbf{I_2}}{\cos\theta_A} \cos\theta \right) e^{-j\theta}. \tag{12}$$

For broadband Doherty operation (second efficiency peak), the saturation value of $\mathbf{V_T}$ has to be maximized over the frequency band of interest. Equations (11) and (12) imply that both the magnitude and phase control of $\mathbf{I_1}$ and $\mathbf{I_2}$ are required. Here, for ease of DPA implementation, only the optimal control of phase is exploited based on the synthesis of matching networks with specific dispersion characteristics. If the phase difference between $\mathbf{I_1}$ and $\mathbf{I_2}$ is denoted as θ_Δ, the output current of the auxiliary device can thus be mathematically expressed as

$$\mathbf{I_2} = \begin{cases} 0, & I_1 < 0.51 I_{1sat} \\ (2I_1 - I_{1\mathrm{sat}}) e^{j\theta_\Delta}, & I_1 \geq 0.51 I_{1sat}. \end{cases} \tag{13}$$

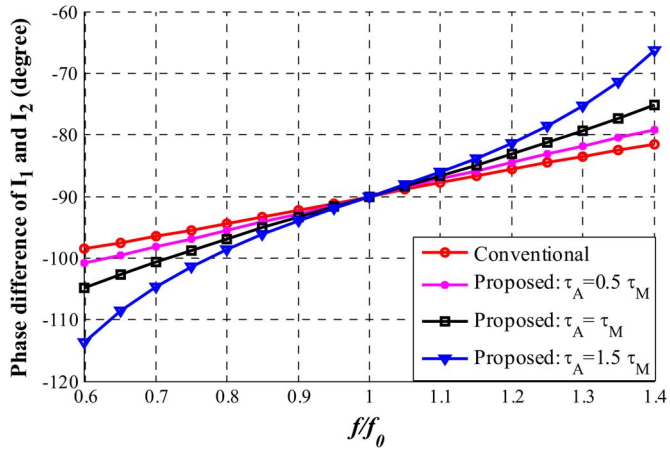

Fig. 4. Calculated phase difference as a function of frequency.

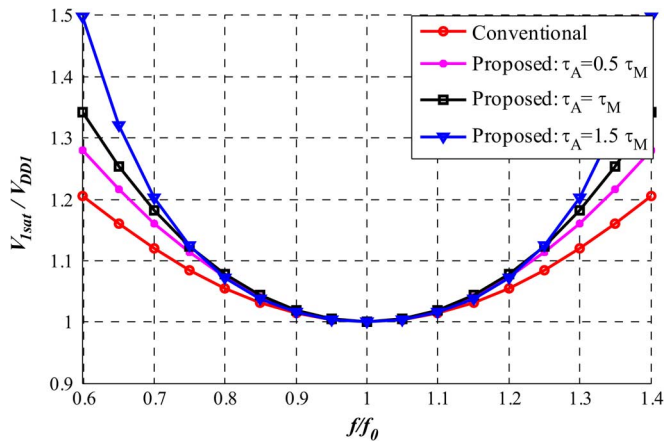

Fig. 5. Saturation drain voltage of main device versus frequency.

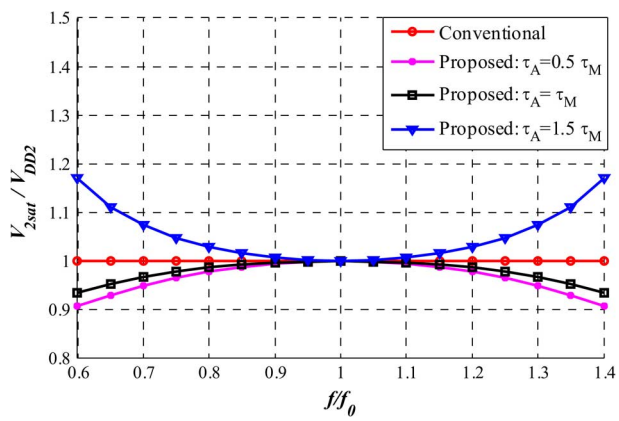

Fig. 6. Saturation drain voltage of auxiliary device versus frequency.

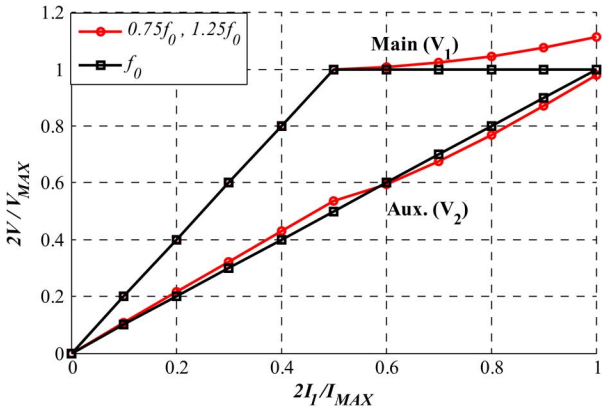

Fig. 7. Calculated drain voltage of proposed topology.

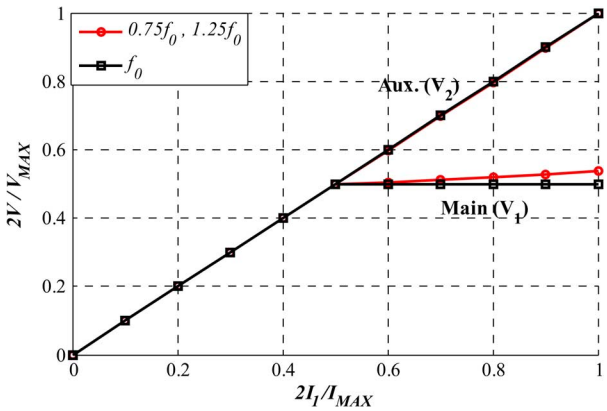

Fig. 8. Calculated drain voltage of conventional topology.

By inserting (13) into (12), the value of $\mathbf{V_T}$ at saturation is simply given by

$$\mathbf{V_{Tsat}} = I_{1\text{sat}} R_{\text{opt}} \left(2 + \frac{\cos\theta}{\cos\theta_A} e^{j\theta_\Delta}\right) e^{-j\theta}. \quad (14)$$

Based on the criteria of maximum output power (i.e., $|\mathbf{V}_{T\text{sat}}| = V_{\text{MAX}} = 2I_{1\text{sat}}\ R_{\text{opt}}$), the optimal phase difference can be deduced from (14) and written as

$$\cos(\theta_\Delta) = -\frac{\cos(\theta)}{4\cos(\theta_A)}. \quad (15)$$

For illustration, Fig. 4 shows the calculated phase difference as a function of normalized frequency. It is further assumed that θ_M ($= 90°$ at f_0) and θ_A ($= 0°$ at f_0) are both linear functions of frequency with nonzero group delays (τ_M and τ_A). It can be observed that the frequency response of the optimum phase difference strongly depends on the group delay of the auxiliary transformer. For closer examination, Figs. 5 and 6 show the corresponding saturation voltages ($V_{1\text{sat}}$ and $V_{2\text{sat}}$) of the proposed (with auxiliary transformer) and conventional (without auxiliary transformer) designs. In these plots, optimum phase control of $\mathbf{I_1}$ and $\mathbf{I_2}$ (θ_Δ) is enforced to compensate for the frequency dispersion of θ_M and θ_A. It can be seen that both voltage ratios

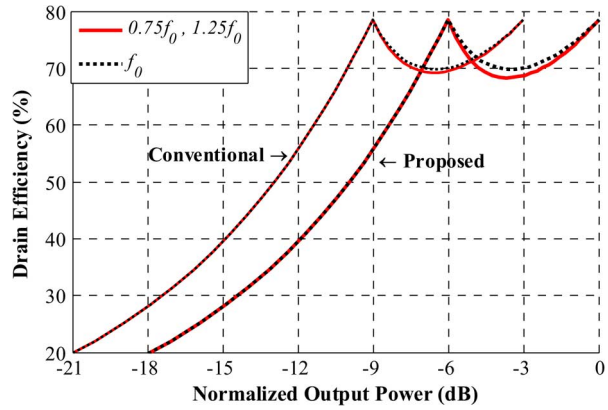

Fig. 9. DE of the proposed and conventional designs.

TABLE I
OPTIMUM DRAIN LOADS OF MAIN AND AUXILIARY DEVICES

Frequency (GHz)	Z_{optcri} (Ω)	Z_{optsat} (Ω)	Z_{optaux} (Ω)
1.6	26.26+52.5j	24.88+37.64j	27.7+39.4j
1.8	24.1+50.4j	24.37+35.67j	25.6+36.6j
2	24.6+48.1j	25.56+31.81j	24.9+32.5j
2.2	24.7+47.3j	24.38+30.71j	24.4+31.3j
2.4	23.8+43.5j	24.38+27.94j	22.8+28.8j

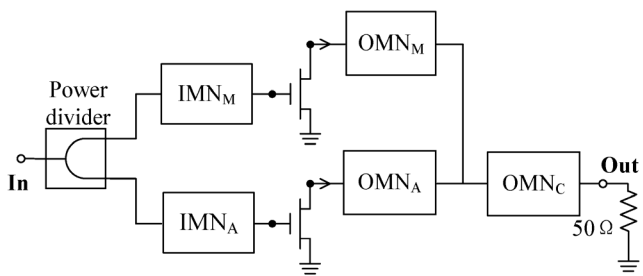

Fig. 10. Block diagram of the proposed DPA.

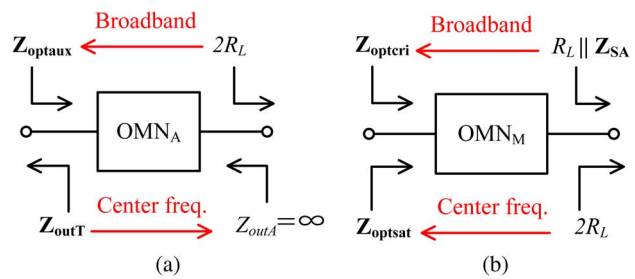

Fig. 11. Design targets of output matching networks. (a) Auxiliary device. (b) Main device.

are normalized to 1 at the center frequency. However, they deviate gradually from unity with increasing offset in frequency. It is because only phase compensation is deliberately applied, but not magnitude control (main and auxiliary currents). Nevertheless, the operating bandwidth is primarily determined by the overdrive of the main device (voltage ratio >1). For instance, with a maximum voltage ratio of 1.1, a fractional bandwidth

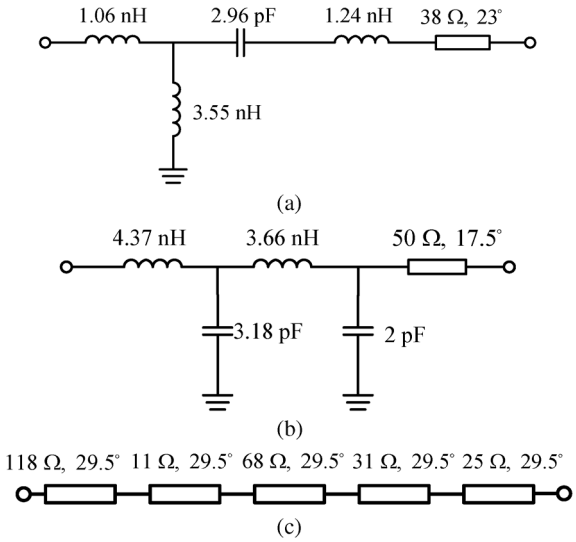

Fig. 12. Circuit topologies for auxiliary matching network. (a) Bandpass. (b) Low-pass 1. (c) Low-pass 2.

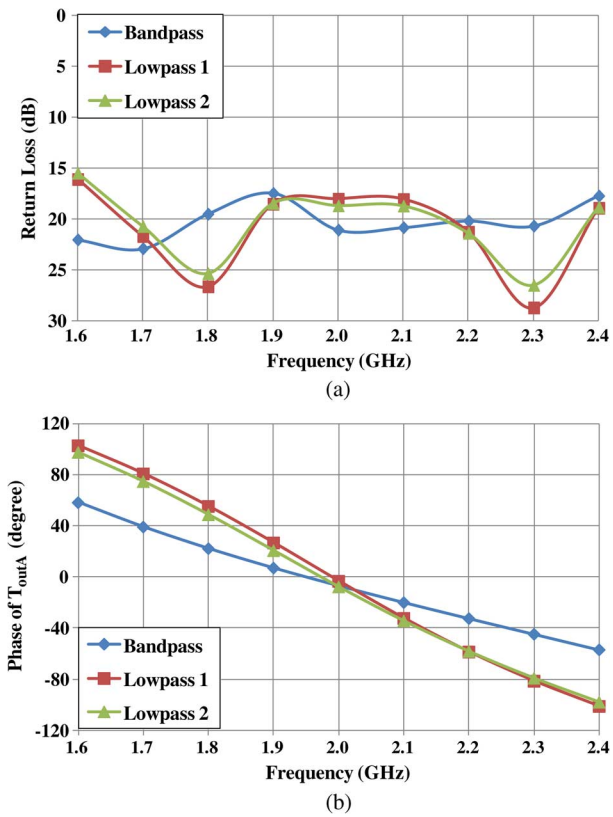

Fig. 13. Simulation results of different circuit topologies. (a) Return loss. (b) Phase response.

(FBW) of about 50% can be achieved. Meanwhile, the available bandwidth diminishes with increasing value of τ_A.

D. Drain Voltage Profiles and Efficiency Performance

Figs. 7 and 8 show the calculated drain voltage profiles as a function of Main current with equal group-delay assumption ($\tau_M = \tau_A$). Both the proposed (with transformer) and conventional (without transformer) DPA configurations were examined

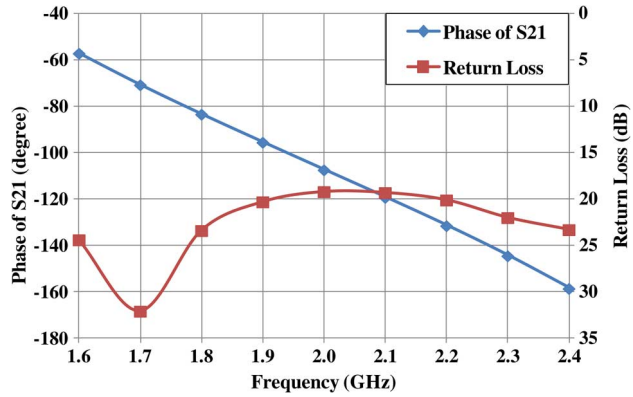

Fig. 14. Simulated return loss and phase response of OMN_M.

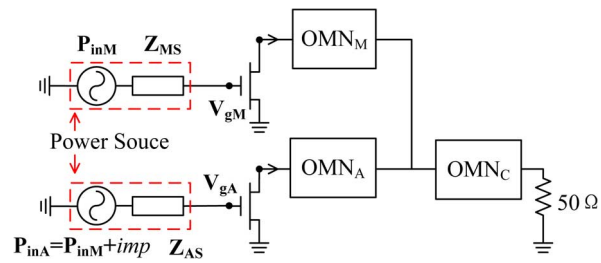

Fig. 15. Circuit configuration for optimal phase extraction.

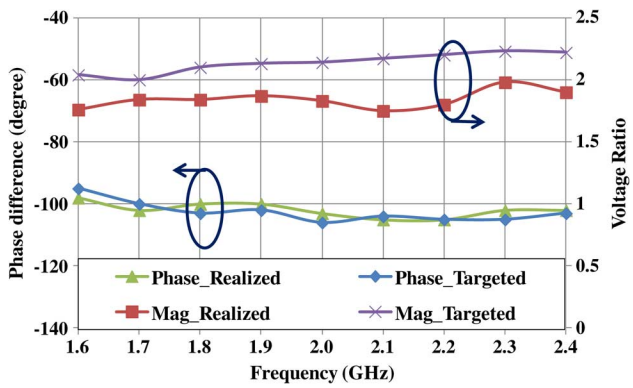

Fig. 16. Extracted and realized voltage ratio and phase difference by simulation.

at the center frequency and band edges ($0.75f_0$, f_0, and $1.25f_0$). It is also assumed that each device is operating at its highest possible rating (saturation voltage and current). In comparison to the conventional circuit, the saturation voltage of the main device in the proposed topology is double over the entire Doherty region due to adoption of a higher drain bias. Meanwhile, the drain voltage profiles of the two auxiliary devices are very similar. At the band edges, the saturation voltage ratio of the main device (proposed) has increased slightly to 1.1, as expected. For further investigation, Fig. 9 illustrates the calculated drain efficiency (DE) of the two DPA configurations. Both designs offer excellent Doherty behavior (OBO range of 6 dB), but the proposed topology can deliver 3 dB more output power than the conventional structure due to the enhancement of the PUF.

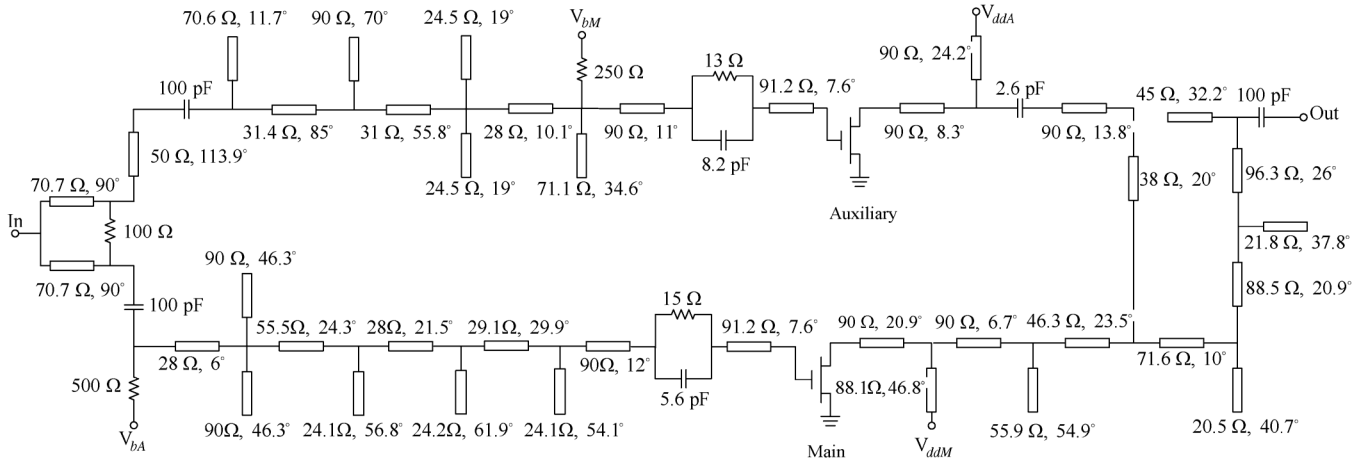

Fig. 17. Schematic diagram of the proposed DPA.

III. Circuit Design and Simulation

A broadband DPA (1.6–2.4 GHz), with targeted output power of 43 dBm and PUF $= 1$, was designed based on the adoption of the auxiliary transformer and optimum phase compensation. All simulations were performed using Agilent Technologies' Advanced Design System (ADS) with a large-signal model of Cree's GaN transistor CGH40006S.

A. Bias Selection and Optimum Drain Load Extraction

According to the device specifications (datasheet), the breakdown voltage (drain–source) of CGH40006S is 120 V. Meanwhile, the drain voltage (peak value) of high-efficiency amplifiers (e.g. Class C, Class J, and Class F) is much larger than the dc bias voltage (2–3 times) [17], [18]. For reliability consideration, the auxiliary drain bias is therefore selected to be 40 V. Furthermore, the adoption of the AB-C Doherty configuration will lead to a slight reduction of the PUF (by a few percent). It is also well known that, to attain ideal Doherty behavior with OBO of 6 dB, it is essential to have a similar level of output power delivered from both the main and auxiliary devices. However, the lower output power capacity of the auxiliary device (Class C) [19] causes insufficient load modulation and results in degradation in efficiency and power performance [20]. This issue is prominent in broadband DPA design as the harmonic tuning of PA is usually more difficult to achieve over wide bandwidth. Subsequently, the drain bias of the main device is deliberately reduced to 35 V for having comparable output power (hence, the theoretical PUF is lowered to around 90%). Under the above bias condition, the optimum drain load impedances (Table I) of the real devices were then extracted by using load–pull simulations. The optimum load impedances ($\mathbf{Z_{optcri}}$ and $\mathbf{Z_{optsat}}$) of the main device were determined at an output power level of 37.5 dBm (6-dB back-off) and 40.5 dBm (saturation). Meanwhile, the optimum load impedance ($\mathbf{Z_{optaux}}$) of the auxiliary device was obtained at an output power of 40.5 dBm (saturation).

B. Design of Output Matching Network of Auxiliary Device

Fig. 10 shows the block diagram of the proposed DPA (biasing circuitry is omitted for clarity). It is well known that the proper selection of the combining load (R_L) can offer extra design freedom to the broadband realization of output matching networks [5]. Based on the design targets outlined in Fig. 11, an optimum value of $R_L (= 19\ \Omega)$ was found by using the simplified real frequency technique (SRFT) [21], [22]. Subsequently, both OMN_A and OMN_M will involve additional impedance transformation from R_L to $2R_{\mathrm{opt}}$.

Referring to Fig. 11(a), the design targets of OMN_A include broadband impedance transformation from the combining load ($2R_L$) to the optimum drain load ($\mathbf{Z_{optaux}}$), as well as the provision of sufficiently high output impedance ($\mathbf{Z_{outA}}$) when the auxiliary device is off. Note that the proposed transformer (Fig. 2) is realized by the combined effect of OMN_A and device parasitic (after the impedance transformation from R_L to $2R_{\mathrm{opt}}$ is de-embedded). Moreover, due to the adoption of different drain bias voltages for the main and auxiliary devices, the voltage ratio of the auxiliary transformer is slightly changed to 1.7:1 (instead of 2:1) to reflect the unequal values of optimum load.

It is well understood that the output impedance of the auxiliary matching network in the off-state is crucial in realizing broadband Doherty behavior. In theory, the output impedance of the matching network should approach infinity (open circuit) when the auxiliary device is off, but in practice, the quasi-open-circuit requirement ($|\mathbf{\Gamma}_{\mathrm{out}A}| \approx 1, -45^\circ < \angle\mathbf{\Gamma}_{\mathrm{out}A} < -45^\circ$) is usually imposed [5]. Hence, apart from fulfilling the purpose of impedance matching, the auxiliary circuit should also exhibit minimal phase variation in the output reflection coefficient [5]. Fig. 12 shows the prototypes under investigation, which include one bandpass and two low-pass topologies. In meeting the design targets, they can be synthesized by SRFT. For comparison purposes, the frequency response of return loss and phase of $\mathbf{\Gamma_{outA}}$ (all prototypes) were simulated and depicted in Fig. 13. Among the three cases, only the bandpass design can offer good matching performance and small phase change. These results indicate that the phase variation of the bandpass design is almost halved with respect to the low-pass counterparts.

C. Output Matching of Main Device and Combining Network

Referring to Fig. 11(b), the major design target of OMN_M is to transform the load impedance from $R_L//\mathbf{Z_{SA}}$ to $\mathbf{Z_{optcri}}$

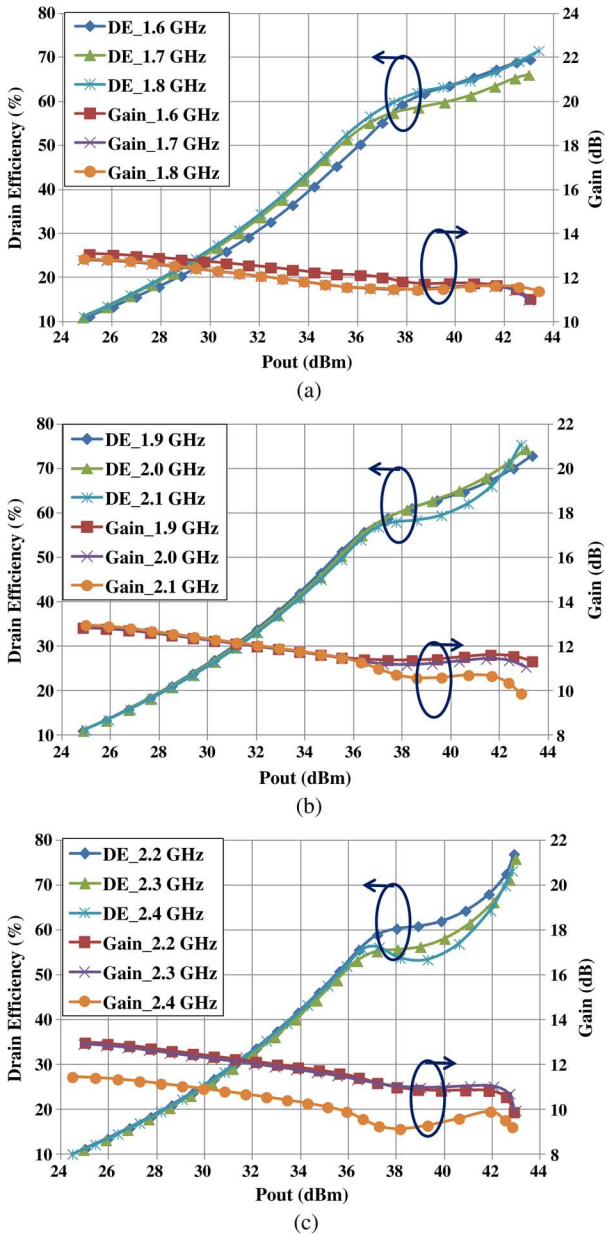

Fig. 18. Simulated DE and gain performance of the proposed DPA. (a) 1.6–1.8 GHz. (b) 1.9–2.1 GHz. (c) 2.2–2.4 GHz.

(auxiliary device is off), and from R_L to $\mathbf{Z_{optsat}}$ (auxiliary device is on). After the impedance transformation from R_L to $2R_{\rm opt}$ is de-embedded, the combined effect of $\rm OMN_M$ and device parasitic should represent an impedance inverter [see Fig. 3(b)] with characteristic impedance of $2R_{\rm opt}$ and phase shift of 90° (center frequency). Fig. 14 shows the simulation results of return loss and the transmission phase of the synthesized matching network. Its group delay is much larger ($\times 3$) than that of an ideal quarter-wavelength transmission line, which is considered to be the major cause of bandwidth reduction [8].

The combining output matching network $(\rm OMN_C)$ is employed to transform the external load (50 Ω) to the required combining load (19 Ω). As mentioned in Section II, the drain voltage of the main device could exceed the safety level at large offset frequency from center, and waveform shaping

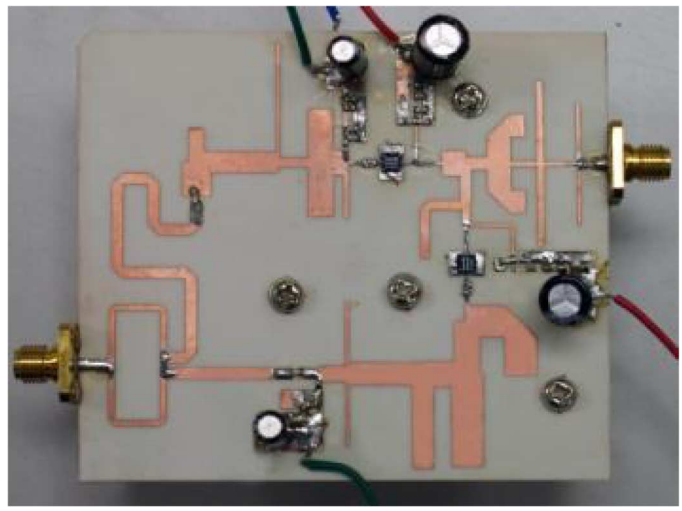

Fig. 19. Photograph of the fabricated DPA.

[17], [18] is often introduced to enhance efficiency and output power. A combining network based on low-pass topology can be designed to provide proper reactive loading (harmonic), as well as impedance matching (fundamental) [23].

D. Extraction of Optimum Phase Difference

In Section II, the optimum condition (phase difference of drain current sources) for enhanced output power and bandwidth is analytically identified. However, in real devices, due to the presence of parasitic capacitance (drain–source), the drain current sources (intrinsic model) are hard to access. Therefore, the gate voltage ratio$(= \mathbf{V_{gA}}/\mathbf{V_{gM}})$ is being monitored instead. With reference to Fig. 15, two voltage sources (main and auxiliary inputs), having controllable magnitude and phase, were employed in the extraction process. The source impedances ($\mathbf{Z_{MS}}$ and $\mathbf{Z_{AS}}$) of the main and auxiliary devices were obtained through source–pull simulation (with optimized gain performance). The gate bias of the main device is set equal to −3 V, which corresponds to a quiescent current of 45 mA (deep Class AB), while the gate bias of the auxiliary device is a free parameter to be determined. Based upon harmonic-balance simulation, at each frequency point, the DE was computed as a function of output power. The gate bias, source impedances, and input signals (both magnitude and phase) were then finely tuned with an aim to optimize the output power, OBO, and efficiency performance. A gate bias (auxiliary) of −7 V and input signals of equal magnitude were subsequently obtained. Finally, based on the extracted source impedances and gate voltage ratio, the input matching networks were synthesized by using the SRFT. Both extracted and realized results of the gate voltage ratio are plotted in Fig. 16, which were found to be approximately 2 (magnitude of voltage ratio) and −105° (phase difference), over the frequency range from 1.6 to 2.4 GHz.

E. Proposed DPA: Simulation Results

Fig. 17 shows the schematic diagram of the final design. A Wilkinson power divider was employed to split the input signal

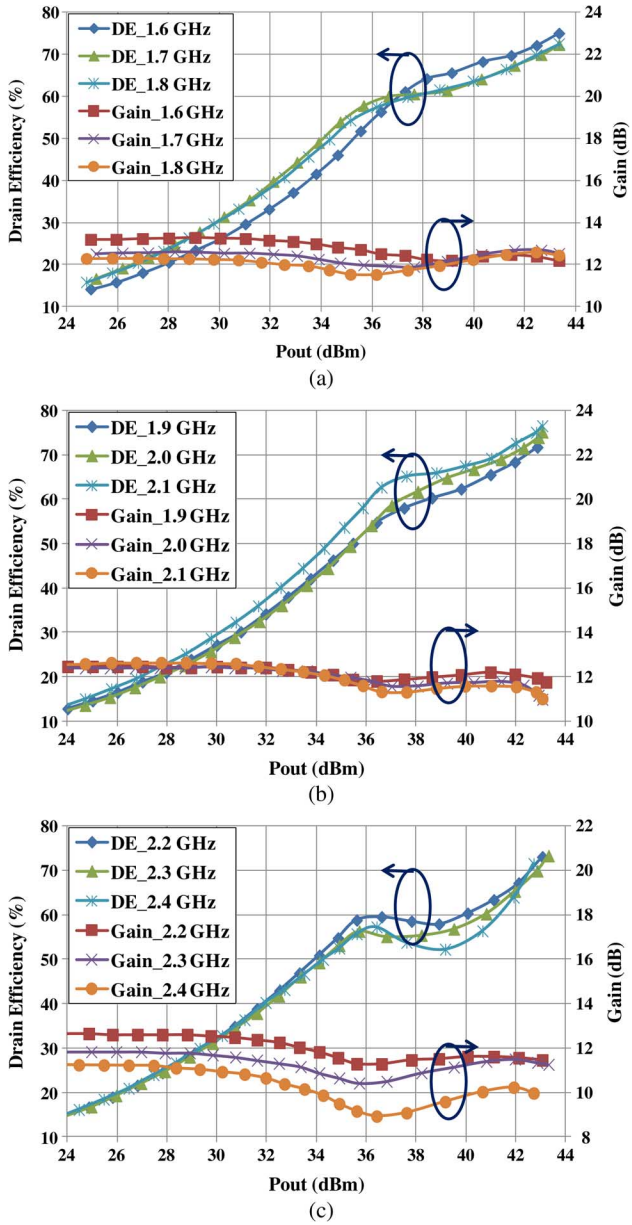

Fig. 20. Measured DE and gain performance of the proposed DPA. (a) 1.6–1.8 GHz. (b) 1.9–2.1 GHz. (c) 2.2–2.4 GHz.

into two equal parts. Both low-pass (input matching, output matching of main device, combining network) and bandpass (output matching of auxiliary device) networks were involved with line impedance ranging from 24 to 96 Ω. For stability control, *RC* circuits were inserted in series connection with the gate inputs of the active devices. To take into account the effect of junction discontinuities and device nonlinearity, co-simulation based upon the large-signal model was conducted. Some fine tuning of the layout was made to further optimize the efficiency and power performance. To minimize the gain variation in the low-power and Doherty regions, the gate bias of the main device (deep Class AB) was slightly modified to give a quiescent drain current of 35 mA while the gate bias of the auxiliary devices (Class C) was readjusted to −6.7 V.

Fig. 18 shows the simulated DE and gain performance as a function of output power. Over the frequency range from 1.6 to

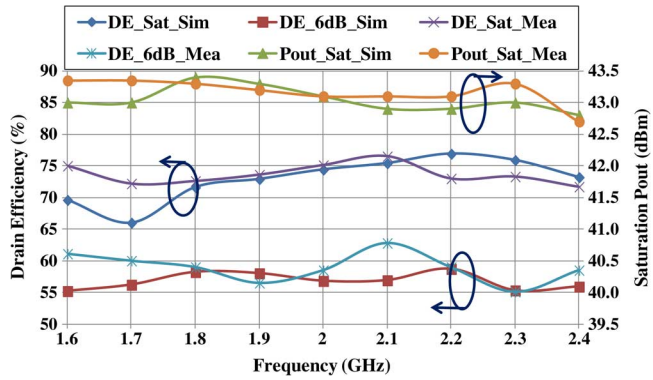

Fig. 21. Variation of DE and output power of proposed DPA as a function of operation frequency. DE_6dB(Sat)_Sim(Mea) represents the simulated (measured) DE at 6-dB back-off (saturation). Pout_Sat_Sim(Mea) represents the simulated (measured) output power at saturation.

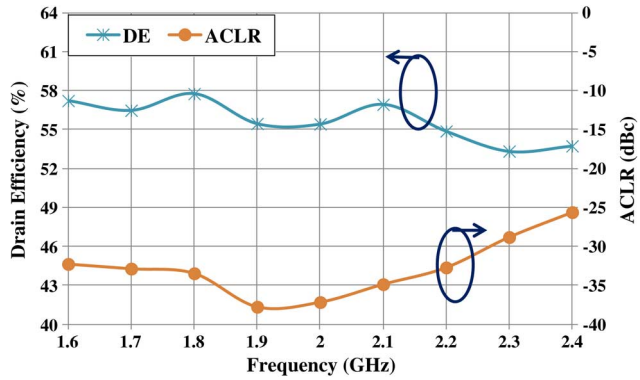

Fig. 22. Measured average DE and ACLR (WCDMA test signal at an average output power of 37 dBm).

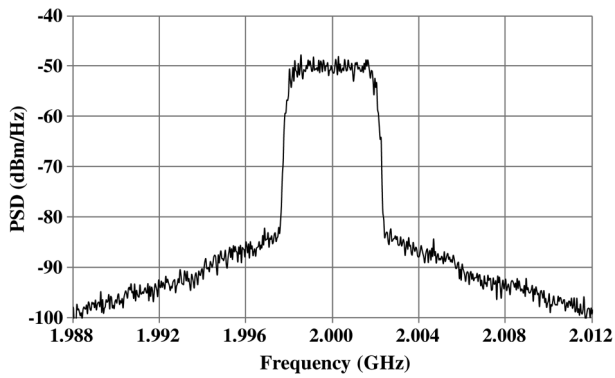

Fig. 23. Measured output spectrum of proposed design (WCDMA test signal at 2 GHz with an average output power of 37 dBm).

2.3 GHz, the saturation output power was found to be close to 43 dBm with the power gain of about 12 dB. Typical Doherty behavior can be observed with a 6-dB back-off efficiency of 55%–64% and saturation efficiency of 68%–76%.

IV. Experimental Verification

For experimental validation, the proposed DPA was fabricated on a microwave substrate (RO4003C) with a thickness of 0.813 mm and a dielectric constant of 3.55. The top view of the prototype is shown in Fig. 19.

TABLE II
COMPARISON OF SOME RECENT BROADBAND DPA DESIGNS BASED ON GaN TECHNOLOGY

	Frequency (GHz)	FBW	DPA Configuration	PUF	OBO (dB)	Saturation Pout (dBm)	DE at Saturation (%)	DE at 6dB back-off (%)	Year
[4]	1.7-2.6	42%	Classical with Low-pass OMN_A	~1	5-6	42.1-45.3	50-55	41-55	2011
[5]	2.2-3.0	31%	Classical with Low-pass OMN_A	~1	5-6	39.4-41.8	55-69	29-53	2012
[6]	1.05-2.55	83%	Modified with Low-pass OMN_A	~1	5-6	40-42	45-83	35-58	2014
[14]*	1.0-3.0	100%	Modified with Low-pass OMN_A	~1	6	43.1-44.9	45-68	48-69	2013
[7]	0.7-1.0	35%	Modified w/o OMN_A	~0.5	6	49-50.8	61-75	52-64	2012
[8]	1.5-2.4	46%	Modified w/o OMN_A	~0.5	6	~ 42	52-68	50-62	2013
This Work	1.6-2.4	40%	Modified with Band-pass Auxiliary Transformer	~0.9	6-7	42.7-43.3	72-77	55-63	2015

*Digital dual Class-B PA using mixed Doherty/outphasing operation, no PUF degradation caused by Class-C operation.

A. Continuous Wave Signal Measurement

Fig. 20 gives the measured gain performance and DE of the proposed DPA as a function of output power under continuous wave (CW) signal stimulation (with frequency ranged from 1.6 to 2.4 GHz in a step of 0.1 GHz). Inside the low-power region, excellent gain flatness (11.5–13 dB) can be observed. Meanwhile, good Doherty efficiency behavior was found from 1.6 to 2.3 GHz with a gain compression of less than 1.5 dB. With reference to Fig. 21, the measured drain efficiencies at saturation (around 43 dBm) and 6-dB power back-off (around 37 dBm) were over 71% and 55%, respectively, for the entire frequency band. Small variation in saturation output power and DE with frequency was clearly observed.

B. Modulated Signal Measurement

To access the efficiency and linearity performance of the proposed DPA under modulated signal stimulation, measurements based upon the single-carrier WCDMA signal with PAPR of 6.6 dB at 0.1% probability of complementary cumulative distribution function (CCDF) were employed. Fig. 22 shows the measured DE and ACLR (with 5-MHz offset) at an average output power of 37 dBm. The ACLR performance was better than -32 dBc from 1.6 to 2.2 GHz. Nevertheless, excellent average DE (53%–58%) can be obtained over the entire band. Fig. 23 shows the output spectrum of the proposed DPA with WCDMA stimulation centered at 2 GHz, which indicates an ACLR level of -37 dBc.

Table II shows the summary of this work and some recent reports on broadband DPA designs with the same device technology. As some of the auxiliary transistors involved were operating under high-efficiency classes (e.g., J and F) with uncertain peak voltage levels, and therefore, in the calculation of the PUF, the drain bias of the device has been adopted as the maximum voltage rating (rather than one-half of the breakdown voltage).

In comparison to conventional approaches [7], [8], it is clear that the PUF can be greatly enhanced (from 0.5 to 0.9) with the introduction of an auxiliary transformer. Besides, the best 6-dB back-off and saturation efficiencies (around 59% and 75%, respectively) have been achieved, which reveals that the proposed method can offer excellent efficiency-bandwidth performance. Especially when compared to [8] and [14], the proposed design is solely based on analog circuitry and no sophisticated digital control is involved. It is also worth mentioning that this work deliberately selects unequal drain bias for the main and auxiliary amplifiers to improve OBO (6–7 dB) and output power variation with frequency (43 ± 0.3 dBm) at the expense of the PUF ($\sim$0.9).

V. CONCLUSION

A new broadband DPA configuration using a bandpass auxiliary transformer to improve the PUF has been presented. The broadband performance of the proposed and conventional topologies has been analytically investigated and compared. Issues relating to the design of the auxiliary transformer and optimum control of phase difference have also been addressed. A prototype of the proposed DPA has been designed, built, and characterized with CW and WCDMA signal formats. These results indicate that the proposed design is capable of providing a high PUF and state-of-the-art efficiency-bandwidth performance.

REFERENCES

[1] W. H. Doherty, "A new high efficiency power amplifier for modulated waves," *Proc. IRE*, vol. 24, no. 9, pp. 1163–1182, Sep. 1936.
[2] S. Cripps, *RF Power Amplifiers for Wireless Communications*, 2nd ed. Norwood, MA, USA: Artech House, 2006.
[3] J. H. Qureshi *et al.*, "A wideband 20 W LMOS Doherty power amplifier," in *IEEE MTT-S Int. Microw. Symp. Dig.*, Anaheim, CA, USA, May 2010, pp. 1504–1507.
[4] K. Bathich, A. Markos, and G. Boeck, "Frequency response analysis and bandwidth extension of the Doherty amplifier," *IEEE Trans. Microw. Theory Techn.*, vol. 59, no. 4, pp. 934–944, Apr. 2011.
[5] G. Sun and R. Jansen, "Broadband Doherty power amplifier via real frequency technique," *IEEE Trans. Microw. Theory Techn.*, vol. 60, no. 1, pp. 99–111, Jan. 2012.
[6] R. Giofre, L. Piazzon, P. Colantonio, and F. Giannini, "A close-form design technique for ultra-wideband Doherty power amplifiers," *IEEE Trans. Microw. Theory Techn.*, vol. 62, no. 12, pp. 3414–3224, Dec. 2014.
[7] Y.-T. Wu and S. Boumaiza, "A modified Doherty configuration for broadband amplification using symmetrical devices," *IEEE Trans. Microw. Theory Techn.*, vol. 60, no. 10, pp. 3201–3213, Oct. 2012.
[8] D. Gustafsson, C. Andersson, and C. Fager, "A modified Doherty power amplifier with extended bandwidth and reconfigurable efficiency," *IEEE Trans. Microw. Theory Techn.*, vol. 61, no. 1, pp. 533–542, Jan. 2013.
[9] Y.-T. Wu and S. Boumaiza, "A mixed-technology asymmetrically biased extended and reconfigurable doherty amplifier with improved power utilization factor," *IEEE Trans. Microw. Theory Techn.*, vol. 61, no. 5, pp. 1946–1956, May 2013.

[10] A. Grebennikov and J. Wong, "A dual-band parallel Doherty power amplifier for wireless applications," *IEEE Trans. Microw. Theory Techn.*, vol. 60, no. 10, pp. 3214–3222, Oct. 2012.
[11] R. Giofrè, L. Piazzon, P. Colantonio, and F. Giannini, "A distributed matching/combining network suitable for Doherty power amplifiers covering more than an octave frequency band," in *IEEE MTT-S Int. Microw. Symp. Dig.*, Tampa, FL, USA, Jun. 2014.
[12] M. N. A. Abadi, H. Golestaneh, H. Sarbishaei, and S. Boumaiza, "An extended bandwidth Doherty power amplifier using a novel output combining," in *IEEE MTT-S Int. Microw. Symp. Dig.*, Tampa, FL, USA, Jun. 2014.
[13] J. H. Qureshi, W. Sneijers, R. Keenan, L. C. N. deVreede, and F. van Rijs, "A 700-W peak ultra-wideband broadcast Doherty amplifier," in *IEEE MTT-S Int. Microw. Symp. Dig.*, Tampa, FL, USA, Jun. 2014.
[14] C. M. Andersson, D. Gustafsson, J. C. Cahuana, R. Hellberg, and C. Fager, "A 1–3-GHz digitally controlled dual-RF input power-amplifier design based on a Doherty-outphasing continuum analysis," *IEEE Trans. Microw. Theory Techn.*, vol. 61, no. 10, pp. 3743–3752, Oct. 2013.
[15] X. Fang and K. M. Cheng, "Extension of high-efficiency range of Doherty amplifier by using complex combining load," *IEEE Trans. Microw. Theory Techn.*, vol. 62, no. 9, pp. 2038–2047, Sep. 2014.
[16] K. Kurokawa, "Power waves and the scattering matrix," *IEEE Trans. Microw. Theory Techn.*, vol. MTT-13, no. 2, pp. 194–202, Mar. 1965.
[17] S. C. Cripps, P. J. Tasker, A. L. Clarke, J. Lees, and J. Benedikt, "On the continuity of high efficiency modes in linear RF power amplifiers," *IEEE Microw. Wireless Compon. Lett.*, vol. 19, no. 10, pp. 665–667, Oct. 2009.
[18] V. Carrubba *et al.*, "On the extension of the continuous class-F mode power amplifier," *IEEE Trans. Microw. Theory Techn.*, vol. 59, no. 5, pp. 1294–1303, May 2011.
[19] P. Colantonio, F. Giannini, R. Giofrè, and L. Piazzon, "The AB-C Doherty amplifier, Part I: Theory," *Int. J. RF Microw. Comput.-Aided Eng.*, vol. 19, no. 3, pp. 293–306, May 2009.
[20] K. Jangheon *et al.*, "Power efficiency and linearity enhancement using optimized asymmetrical Doherty power amplifiers," *IEEE Trans. Microw. Theory Techn.*, vol. 59, no. 2, pp. 425–434, Feb. 2011.
[21] Y. S. Binboga, *Design of Ultra Wideband Power Transfer Networks*. New York, NY, USA: Wiley, 2010.
[22] B. S. Yarman and H. J. Carlin, "A simplified 'real frequency' technique applied to broadband multistage microwave amplifiers," *IEEE Trans. Microw. Theory Techn*, vol. MTT-30, no. 12, pp. 2216–2222, Dec. 1982.
[23] K. Chen and D. Peroulis, "Design of broadband highly efficient harmonic-tuned power amplifier using in-band continuous class-mode transferring," *IEEE Trans. Microw. Theory Techn.*, vol. 60, no. 12, pp. 4107–4116, Dec. 2012.

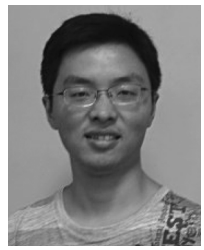

Xiao-Hu Fang (S'12) received the B.Eng. and M.Eng degrees in electronic science and technology from the Huazhong University of Science and Technology, Hubei, China, in 2008 and 2011, respectively, and the Ph.D. degree in electronic engineering from The Chinese University of Hong Kong, Shatin, Hong Kong, in 2015.

He is currently a Research Assistant with the Department of Electronic Engineering, The Chinese University of Hong Kong. His current research interests include the design of advanced high-efficiency power amplifiers and associated linearization methods.

Kwok-Keung M. Cheng (S'90–M'91–SM'06) received the B.Sc. degree (first-class honors) and Ph.D. degree in electronic engineering from King's College, University of London, London, U.K., in 1987 and 1993, respectively.

In 1996, he joined the Department of Electronic Engineering, The Chinese University of Hong Kong, Shatin, Hong Kong, as an Assistant Professor, becoming an Associate Professor in 2001, and a Professor in 2006. From 2004 to 2006, he was the Associate Dean of Engineering (Student Affairs), The Chinese University of Hong Kong. He has been the lead author of over 20 technical papers published in the IEEE TRANSACTION IN MICROWAVE THEORY AND TECHNIQUES. He was a contributing author of *MMIC Design* (IEE Press, 1995) and *RFIC and MMIC Design and Technology* (IEE Press, 2001). His current research interests include the design of monolithic microwave integrated circuits, high-efficiency power amplifiers, multi-band circuits, and reconfigurable devices for advanced applications.

Dr. Cheng is a Chartered Engineer (Institution of Engineering and Technology). From 2008 to 2012, he was an associate editor for the IEEE MICROWAVE AND WIRELESS COMPONENTS LETTERS. He was the recipient of the 1988 Convocation Susquicentennial Prize in Engineering presented by the University of London.